ORIGINAL ARTICLE

Micro–Computed Tomography Comparison of Preterminal Bronchioles in Centrilobular and Panlobular Emphysema

Naoya Tanabe[1], Dragoş M. Vasilescu[1], John E. McDonough[1,2], Daisuke Kinose[1], Masaru Suzuki[1,3], Joel D. Cooper[4], Peter D. Paré[1], and James C. Hogg[1]

[1]Centre for Heart and Lung Innovation, St. Paul's Hospital, University of British Columbia, Vancouver, British Columbia, Canada; [2]Department of Clinical and Experimental Medicine, Division of Respiratory Diseases, KU Leuven–University of Leuven, Leuven, Belgium; [3]First Department of Medicine, Hokkaido University School of Medicine, Sapporo, Japan; and [4]Division of Thoracic Surgery, University of Pennsylvania, Philadelphia, Pennsylvania

Abstract

Rationale: Very little is known about airways that are too small to be visible on thoracic multidetector computed tomography but larger than the terminal bronchioles.

Objectives: To examine the structure of preterminal bronchioles located one generation proximal to terminal bronchioles in centrilobular and panlobular emphysema.

Methods: Preterminal bronchioles were identified by backtracking from the terminal bronchioles, and their centerlines were established along the entire length of their lumens. Multiple cross-sectional images perpendicular to the centerline were reconstructed to evaluate the bronchiolar wall and lumen, and the alveolar attachments to the outer airway walls in relation to emphysematous destruction in 28 lung samples from six patients with centrilobular emphysema, 20 lung samples from seven patients with panlobular emphysema associated with alpha-1 antitrypsin deficiency, and 47 samples from seven control (donor) lungs.

Measurements and Main Results: The preterminal bronchiolar length, wall volume, total volume (wall + lumen), lumen circularity, and number of alveolar attachments were reduced in both centrilobular and panlobular emphysema compared with control lungs. In contrast, thickening of the wall and narrowing of the lumen were more severe and heterogeneous in centrilobular than in panlobular emphysema. The bronchiolar lumen was narrower in the middle than at both ends, and the decreased number of alveolar attachments was associated with increased wall thickness in centrilobular emphysema.

Conclusions: These results provide new information about small airways pathology in centrilobular and panlobular emphysema and show that these changes affect airways that are not visible with thoracic multidetector computed tomography scans but located proximal to the terminal bronchioles in chronic obstructive pulmonary disease.

Keywords: computed tomography; small airway; imaging; chronic obstructive pulmonary disease

Disease in the small conducting airways less than 2 mm in diameter and emphysematous destruction are major pathologic features of chronic obstructive pulmonary disease (COPD) (1). The relative contribution of these two processes varies across individuals and emphysematous destruction is further categorized based on its morphology: centrilobular emphysema (CLE), panlobular emphysema (PLE), and paraseptal emphysema (1–3). These pathologic features underlie various clinical and radiographic manifestations in COPD and, in particular, CLE and PLE have been recognized as distinct pathologic phenotypes (3–6). Histologic comparisons have shown that emphysematous destruction is more heterogeneous and

(Received in original form February 10, 2016; accepted in final form September 9, 2016)

Supported by the National Institutes of Health (R01 HL122438), Canadian Institutes of Health Research (Thoracic Imaging Network of Canada), and investigator-initiated contracts from the Grifols and Respivert corporations.

Author Contributions: N.T., design of study, development of a program to analyze bronchioles on microCT images, analysis of data, and writing draft. D.M.V., design of study, tissue procurement, intellectual contributions, and manuscript editing. J.E.M., tissue procurement and microCT acquisitions. D.K., design of study and intellectual contributions. M.S., tissue procurement and measurement of airway wall on histology. J.D.C., tissue procurement. P.D.P., intellectual contributions and manuscript editing. J.C.H., conception and design of study, intellectual contributions, and manuscript editing.

Correspondence and requests for reprints should be addressed to James C. Hogg, M.D., Ph.D., Centre for Heart and Lung Innovation, St. Paul's Hospital, University of British Columbia, 166-1081 Burrard Street, Vancouver, BC, V6Z 1Y6 Canada. E-mail: jim.hogg@hli.ubc.ca

This article has an online supplement, which is accessible from this issue's table of contents at www.atsjournals.org

Am J Respir Crit Care Med Vol 195, Iss 5, pp 630–638, Mar 1, 2017

Originally Published in Press as DOI: 10.1164/rccm.201602-0278OC on September 9, 2016
Internet address: www.atsjournals.org

At a Glance Commentary

Scientific Knowledge on the Subject: Although multidetector computed tomography has been used to study small airways of approximately 2 mm in diameter and micro–computed tomography has been used to study terminal bronchioles of approximately 400–500 μm in diameter, very little is known about the smaller bronchi and bronchioles between these two locations.

What This Study Adds to the Field: This report provides new information about the abnormalities in the preterminal bronchioles of patients with panlobular emphysema associated with alpha-1 antitrypsin deficiency and patients with centrilobular emphysema commonly associated with cigarette smoking.

small airway disease is more severe in CLE than in PLE (4, 5, 7).

The introduction of computed tomography (CT) and the rapid development of multidetector CT (MDCT) imaging has made it possible to obtain high-quality images of the entire thorax during a single breathhold (8). This imaging technique has been widely used to describe and quantify all of the classic pathologic phenotypes of emphysematous destruction in COPD (3, 6, 9) and to measure the changes in lumen and wall of airways 2 mm in diameter and larger (10–12). Although new-generation CT scanners have the potential for greater resolution without an increase in radiation dose (13, 14) and may enable measurements of airways less than 2 mm in diameter, it is not currently possible to resolve the small conducting airways down to the level of the terminal bronchioles. Parametric response map analysis of inspiratory and expiratory MDCT scans has been established to estimate the presence of small airway disease separately from emphysematous destruction (15). Reports using the parametric response map approach have suggested that regions of the lung affected by functional small airway disease develop emphysematous destruction over time (15, 16). These observations are consistent with the microCT results reported by McDonough and coworkers (17) that showed extensive destruction of terminal bronchioles before the onset of emphysematous destruction in explanted lung specimens from patients with severe COPD treated by lung transplantation (17). Although parametric response map provides information about the functional state of small airways that are below the resolution of MDCT, their three-dimensional morphometry has not been systematically investigated with higher resolution imaging tools, such as microCT.

This report begins to investigate the small conducting airways between those visible on MDCT and the terminal bronchioles that are only visible with microCT. Using a novel method to define, orient, and reconstruct the microCT images of small airways, the microstructure of the bronchioles immediately proximal to the terminal bronchioles (preterminal bronchioles) was evaluated quantitatively in the CLE and PLE phenotypes in relation to the severity and heterogeneity of emphysematous destruction surrounding these airways and to the number of alveolar attachments to their outer walls.

Methods

Informed Consent

Informed consent was obtained from patients with COPD waiting for lung transplantation and from the donor's next of kin under conditions that organs unsuitable for transplantation were released for research.

MicroCT Scan

This study is based on microCT scans of 175 lung samples in a previous report on terminal bronchioles in COPD (17) and 64 new samples. At least one complete preterminal bronchioles was identified in 28 samples from six patients with CLE, 20 samples from seven patients with PLE associated with alpha-1 antitrypsin deficiency, and 47 samples from seven donor lungs that served as control lungs. Tissue preparation for microCT imaging has been previously reported in detail (17) and is described in the online supplement (*see* Section E1). Briefly, cores of tissue 14 mm in diameter and 2 cm in length were taken from transverse slices of air-inflated frozen explanted lungs. The cores were fixed at −80°C; warmed to room temperature; dried; and imaged at spatial resolution 10, 11, or 16.4 μm/voxel using microCT scanners (explore Locus SP MicroCT [GE Healthcare, Chicago, IL], Scanco MicroCT35 [Scanco Medical, Brüttisellen, Switzerland], MicroXCT-400 [Zeiss, Oberkochen, Germany], or HMX 225ST [Nikon Metrology, Leuven, Belgium]).

Examination of the Preterminal Bronchioles

Preterminal bronchioles, defined as the airway branch one generation proximal to the terminal bronchioles, were identified by tracking back from terminal bronchioles (17), and subsequently segmented three dimensionally using the ITK-SNAP tool (http://www.itksnap.org/) (18). The centerline down the bronchiole lumen was established using the Skeletonize(2D/3D) plug-in provided in the ImageJ program (National Institutes of Health, Bethesda, MD) (Figure 1A) (19, 20). A custom-designed program generated a series of cross-sectional images perpendicular to the centerline at regular intervals (Figure 1B). Images near the branch points in which either the parent or daughter branches would be visible were excluded (Figure 1C). Bronchiolar length was measured along the centerline and 10 images were selected using a systematic uniform random sampling procedure (*see* Figure E1 in the online supplement) (21).

For each image, the airway wall was segmented based on the full width at half-maximum principle (Figure 1D) (10–12, 22), and the luminal area (Ai), total area (Ao), luminal perimeter (Pi), and outer perimeter (Po) were measured. Internal diameter (ID), wall thickness (WT), wall area (WA), wall area percent (WA%), and circularity of lumen were calculated as $ID = 2\sqrt{Ai/\pi}$, $WT = \sqrt{Ao/\pi} - ID/2$, $WA = Ao - Ai$, $WA\% = 100 \times WA/Ao$, and $circularity = 4\pi(Ai/Pi^2)$, respectively. The number of alveolar attachments (AA#) was counted using a method designed for histology (Figure 1E) (23–25). The perimeter-adjusted number of attachments was calculated as AA#/Po.

For each bronchiole, measurements from the 10 cross-sectional images were averaged. The coefficients of variance (CV[%]) of Ai and WT were calculated to evaluate within-bronchiole and between-bronchioles variabilities. Wall and total

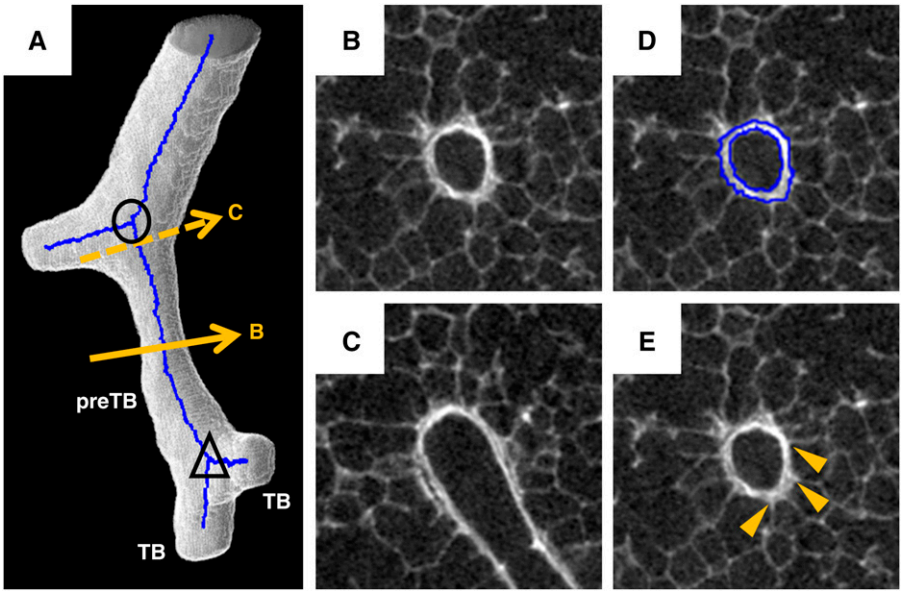

Figure 1. Schematic explanation of preterminal bronchiolar assessment. (*A*) Three-dimensionally segmented preterminal bronchiole (*gray scale*) with centerline identified (*blue*). The *circle* and *triangle* indicate the proximal and peripheral ends of the centerline of the preterminal bronchiole, respectively. PreTB = preterminal bronchiole; TB = terminal bronchiole. (*B*) Cross-sectional image generated perpendicular to the centerline. (*C*) Image near a branch point, which was excluded from this study. (*D* and *E*) Segmentation of the airway wall and examples of alveolar attachments to the outer wall (*arrowheads*), respectively.

airway volume (wall + lumen) were estimated by multiplying the mean WA and Ao by bronchiolar length, respectively.

Quantification of Emphysema

Interalveolar wall distances were measured on 10 images selected from each core based on systematic uniform random sampling (21, 26), and the mean (Lm) and CV% of the interalveolar wall distances were calculated (4, 7).

Statistical Analysis

Linear mixed-effects model that used cases as random effects and Tukey multiple comparison test were performed using the R statistical program (27–29).

Results

Characteristics of patients are provided in Table 1. The ratios of male in control subjects, patients with CLE, and those with PLE were 57%, 50%, and 57%, respectively. All patients with CLE and PLE were former smokers, but the mean value for pack-years was greater in CLE than PLE. One randomly selected preterminal bronchiole was analyzed in each of the 95 tissue cores. Table 2 shows that the ID of all preterminal bronchioles was less than 1 mm. The bronchiolar length was decreased and Lm was increased in CLE and PLE compared with control lungs. The CV% of interalveolar wall distances, a marker of the spatial heterogeneity of emphysematous destruction, was greater in CLE than in PLE and control subjects.

Figure 2 shows a representative microCT image and 10 reconstructed cross-sectional images of a preterminal bronchiole from control (*A*), CLE (*B*), and PLE (*C*) to demonstrate the catenoid shape of the airways in control and CLE, and the thickened wall and narrowed lumen in CLE. To determine if there were any structural abnormalities that varied systematically along the airways' length, the 10 cross-sections from each preterminal bronchiole were separated into three parts where the first proximal part contained images 1–3, the second (middle) part contained images 4–7, and the third peripheral part contained images 8–10 (*see* Figure E2A). The luminal area was decreased in the middle segment of the airways compared with both ends in control subjects and CLE, but not in PLE (*see* Figures E2B–E2D).

Figure 3A shows that the luminal area and total airway area (lumen area + WA) of the preterminal bronchioles were reduced in CLE compared with PLE and control, whereas the WA did not differ among the three groups. Figure 3B shows that the mean WT was increased in CLE compared with PLE and control. The WA% in CLE was also greater than in PLE and control (*see* Figure E3). In contrast, wall volume and total airway volume (wall + lumen) were decreased in both CLE and PLE compared with control subjects (Figure 3C).

Figures 3D and 3E show that the CV% of luminal area and WT within bronchioles was greater in CLE than in control subjects and PLE. The between-bronchioles CV% for luminal area was greater in CLE compared with the other groups and the CV% for WT tended to be greater in these lungs.

Table 1. Patient Characteristics

	Control Subjects ($n = 7$)	Centrilobular Emphysema ($n = 6$)	Panlobular Emphysema ($n = 7$)
Age	56 ± 7	59 ± 3	49 ± 10
Sex, male:female	4:3	3:3	4:3
Height, cm	175 ± 5	170 ± 6	17 ± 8
Weight, kg	79 ± 19	57 ± 12	70 ± 15
Smoking history, never:former	2:5	0:6	0:7
Pack-years in former smokers	32 ± 11*	50 ± 19†	16 ± 6
FEV_1 % predicted	NA	21 ± 6	18 ± 5

Definition of abbreviation: NA = not available.
Data are expressed as mean ± SD per sample.
*The value from two former smokers because pack-year smoking history in three control former smokers is unknown.
†$P < 0.05$ versus panlobular emphysema (Tukey multiple comparison test).

Table 2. Basic Characteristics of Lung Tissue Samples

	Control Subjects ($n = 7$)	Centrilobular Emphysema ($n = 6$)	Panlobular Emphysema ($n = 7$)
Samples, n	47	28	20
Preterminal bronchiole, mm			
Length	2.17 ± 0.78	1.56 ± 0.62*	1.12 ± 0.5*
Internal diameter	0.57 ± 0.11	0.28 ± 0.12*†	0.52 ± 0.17
Emphysema			
Lm, μm	336 ± 37	766 ± 259*	698 ± 240*
CV% of interalveolar wall distance, %	68 ± 7	98 ± 17*†	73 ± 8

Definition of abbreviations: CV% = coefficient of variation expressed as percent (SD/mean × 100); Lm = mean of interalveolar wall distances.
Data are expressed as mean ± SD per sample. One preterminal bronchiole was analyzed for each sample.
*$P < 0.01$ versus control.
†$P < 0.01$ versus panlobular emphysema (Tukey multiple comparison test).

Figure 4A shows that the circularity of the lumen was similarly decreased in CLE and PLE compared with control subjects. The mean number of alveolar attachments per cross-section (Figure 4B) and the number of attachments adjusted by the outer perimeter of the bronchiole (Figure 4C) were decreased in CLE and PLE compared with control subjects, but the extent of the decreases did not differ between CLE and PLE. Table 3 shows that a reduction of the number of alveolar attachments was related to decreased ID in all groups (Figure 4D) (CLE, standardized beta [β*] = 0.59, $P = 0.0006$; PLE, β* = 0.62, $P = 0.002$; and control, β* = 0.72, $P = 0.000004$). In contrast, the decreased numbers of alveolar attachments (Figure 4E) with and without adjustment for outer perimeter length were associated with the increased WT in CLE (β* = −0.61, $P = 0.0008$, and β* = −0.62, $P = 0.0003$, respectively) but not in PLE or control. Lm and CV% of interalveolar wall distances were not associated with WT in any group.

Discussion

A major advantage of microCT over histology is that microCT provides three-dimensional information that can only be obtained by serial reconstruction of two-dimensional images provided by histology. This advantage makes it possible to identify terminal bronchioles anatomically by observing alveoli opening from their walls (15). The present report extends these observations by precisely establishing the position of the preterminal bronchioles (Figure 1) and reconstructing cross-sectional images along their entire length (Figure 2). These results show that in control lungs the preterminal bronchioles have a catenoid shape (i.e., are narrower in the middle than at either end) and that this catenoid shape is accentuated in centrilobular and lost in panlobular emphysematous phenotype of COPD.

The comparisons of the preterminal bronchioles from control lungs with those observed in CLE and PLE (Figure 3) substantially extend the previous histologic findings (2, 5, 7, 17) by showing that the lumen and total (wall + lumen) areas decrease and the WT increases in cross-sections of preterminal bronchiole in centrilobular compared with either PLE or the control subjects (Figures 3A and 3B). The result also shows that despite the increase in WT, WA is not changed. This can be explained by the greater fractional reduction in internal airway diameter than outer airway diameter in CLE.

Furthermore, the direct measurements of preterminal bronchiolar lengths show that these airways were 28% shorter in centrilobular and 48% shorter in PLE compared with control subjects (Table 2). This measurement of airway length also allows for the volume estimation of airway compartments. The results show that the wall volume and total airway volume (wall + lumen) are decreased in both these phenotype of COPD (Figure 3C).

This reduction in preterminal bronchiolar length in COPD (Table 2) is not easy to explain. Because lungs affected by COPD tend to be larger than normal lungs due to loss of lung elastic recoil, the airways embedded in the lung tissue would be expected to elongate as the lung inflates and their length should increase by the cube root of lung volume. In fact, the measured lung volumes were 33% larger in CLE (3.94 ± 1.20 L) and 46% larger in PLE (4.32 ± 1.45 L) emphysema compared with control lungs (2.97 ± 0.61 L). Therefore, this 33% increase in lung volume in CLE and 46% increase in lung volume in PLE should have increased airway length by 3.2% in CLE and 3.6% in PLE, respectively. One possible explanation for this finding was offered by Mitzner in an editorial (30) that accompanied an earlier report on the microCT of terminal bronchioles (17). Mitzner suggested that disruption of the longitudinal bundles of elastic fibers that run the entire length of the airway tree from the trachea to the smallest airways (31) might produce axial retraction and shortening of the airway tree (30).

Figures 3D and 3E show that there is more variability in luminal area and WT of preterminal bronchioles in CLE than PLE. Greater heterogeneity in parenchyma destruction, as evidenced by an increase in the CV% of interalveolar wall distances, has been previously reported in CLE (4, 5, 7) and was present in this study with relatively small sample size (Table 2). CLE is known to be related to the deposition of inhaled particles, such as cigarette smoke (6, 32). As the movement of gas shifts from bulk flow to diffusion in the transitional region of the airways (33), it is a reasonable assumption that the deposition of the smaller airborne particles will target this region of the lung because particles diffuse much more slowly than gases. Thus, the present findings suggest that preterminal bronchioles are included in these transitional regions and the deposition of inhaled small particles is heterogeneously distributed in preterminal bronchioles.

Previous histologic studies have shown the loss of alveolar attachments in emphysematous lungs associated with cigarette smoking (23, 24). Our results extend this finding by showing that the number of alveolar attachments to preterminal bronchioles is decreased both in CLE and PLE relative to control subjects, but the extent of the loss is not different between the two phenotypes (Figure 4). Furthermore, the results extend an earlier histology-based report (34) by showing that the reduction in

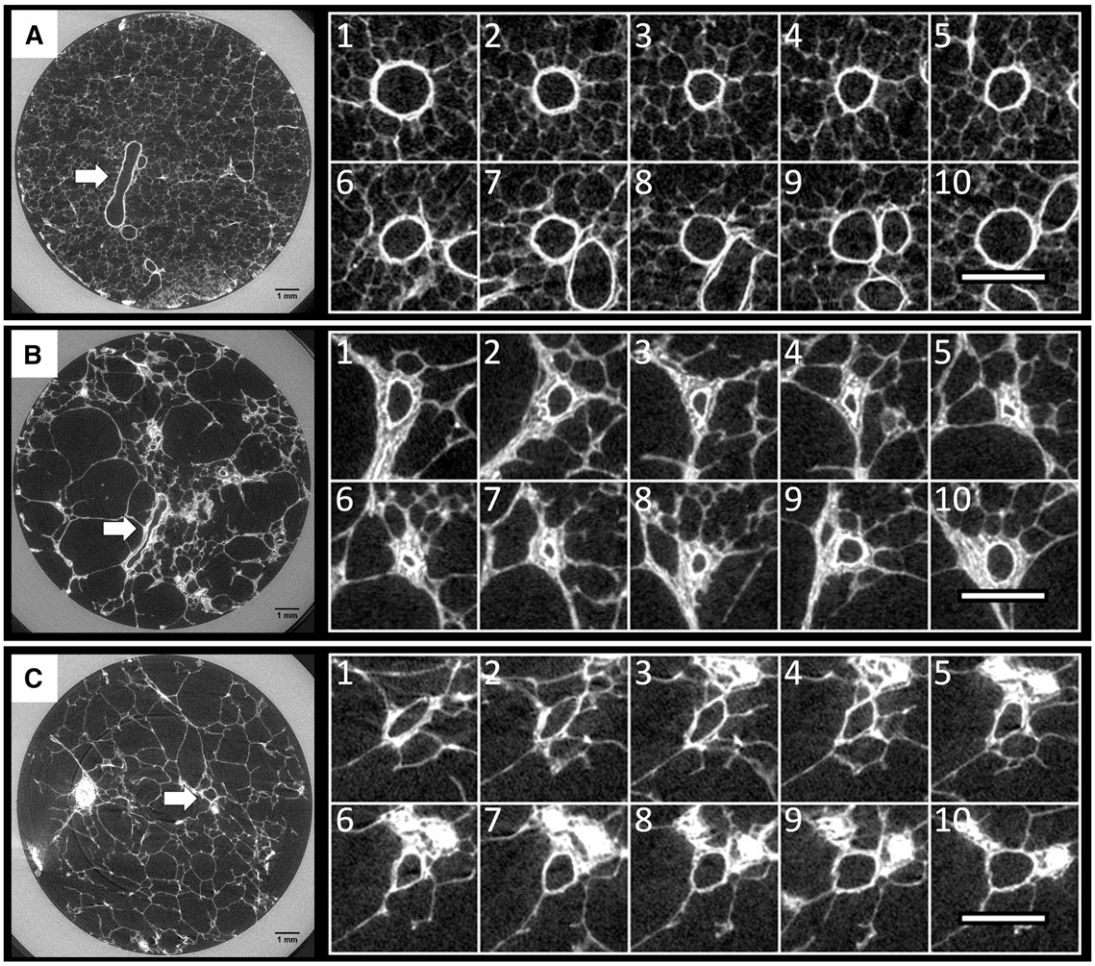

Figure 2. Representative original micro–computed tomography image (*left*) and 10 reconstructed cross-sectional images from one preterminal bronchiole (*right*) from a control lung (*A*) and a lung affected by either centrilobular (*B*) or panlobular (*C*) emphysema. Each *arrow* indicates the location of the preterminal bronchiole. *Scale bars* indicate 1 mm.

number of alveolar attachments correlated with a thicker airway wall in centrilobular but not in panlobular phenotype of emphysema. In contrast, they show that neither Lm nor the CV% of interalveolar wall distances correlated with WT in either phenotype of emphysema. Collectively, these data suggest that small airway disease in CLE is closely associated with peribronchiolar destruction of the parenchyma rather than generalized destruction that includes regions far from the bronchioles. Based on these and other findings (2, 4, 7), we speculated that the pathogenesis of CLE begins with inflammation, remodeling, and destruction of the small airways, with subsequent spread into the peribronchiolar alveolar wall tissue and destruction of the center of the lobule.

In comparison with control lungs, the luminal shape of preterminal bronchioles was deformed in both phenotypes of COPD (Figure 4A). The association between a decreased number of alveolar attachments and reduction in the circularity of their lumens (Table 3) suggests that the loss of alveolar attachments causes reduced radial traction of the small airway and contributes to the distortion of the shape of the lumen (*see* Section E2–1).

Our data showed that preterminal bronchioles in CLE and control subjects have a catenoid shape where the lumen is narrowed in the middle of the segment and widened toward both ends. This catenoid shape disappeared in PLE (Figure 2; *see* Figure E2). We speculate that airway wall thickening in CLE could help to maintain the catenoid shape by mitigating the influence of reduced radial traction caused by loss of alveolar attachments.

There were distinct structural differences in the preterminal bronchioles of CLE and PLE; although the bronchioles in both phenotypes were shorter, were equally noncircular, and had a similar decrease in the number of alveolar attachments, they were narrower and thicker in CLE than in PLE. This comparison of centrilobular form of emphysematous destruction most closely associated with smoking to the evenness of the lobular destruction observed in patients with a genetic deficiency in alpha-1 antitrypsin is of interest. Several previous histology-based reports have shown that the inflammatory immune cell infiltration of the smaller conducting airways is more prominent in CLE than in PLE (4, 5, 35). In contrast, a recent study by Baraldo and coworkers (36) reported the striking observation that there is no difference in either the inflammatory immune cell

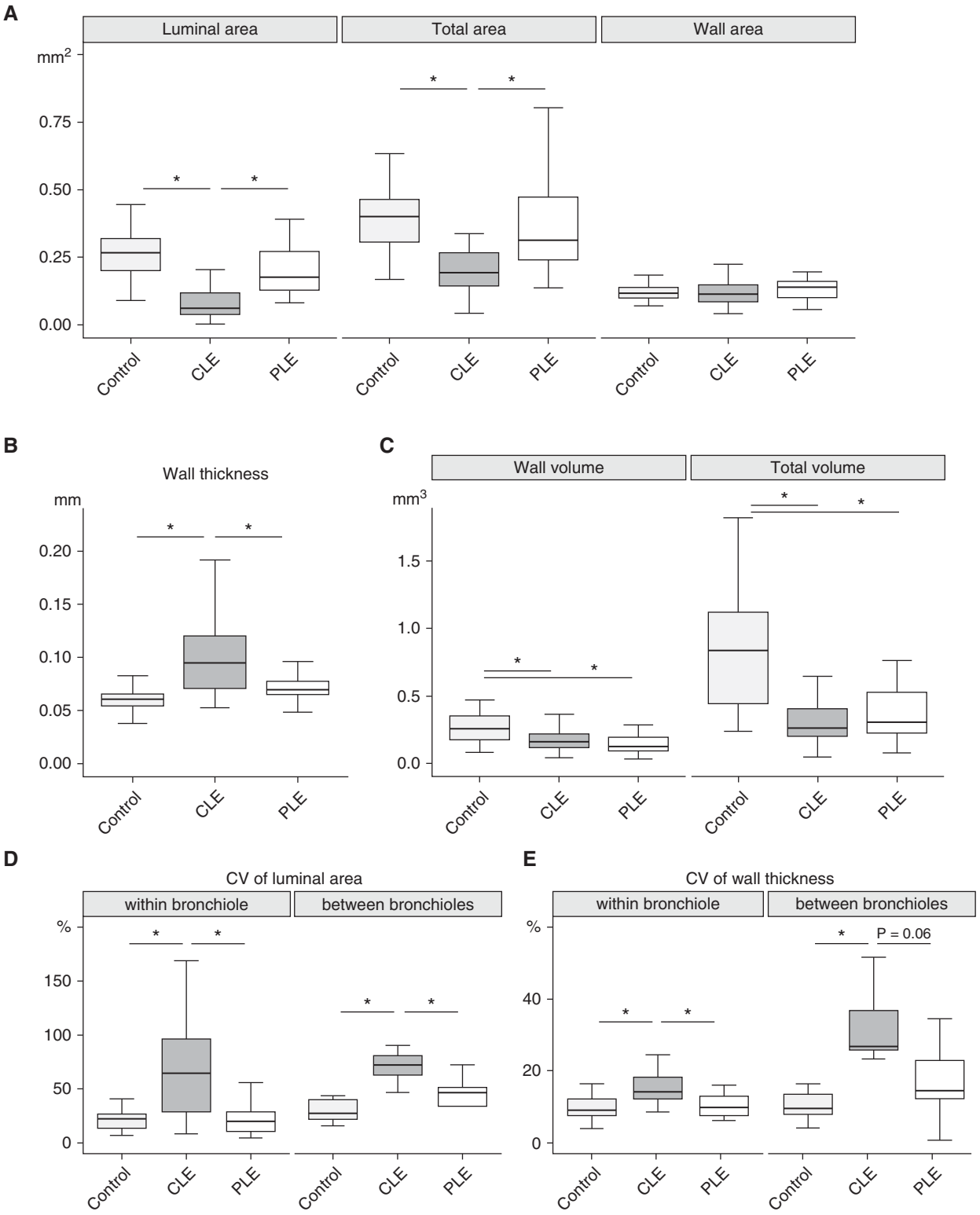

Figure 3. Micro–computed tomography measurements obtained using the methods illustrated in Figures 1 and 2. (*A*) Mean luminal area, total airway area (i.e., lumen + wall) were reduced in centrilobular emphysema (CLE) compared with panlobular emphysema (PLE) and control subjects, but mean wall area did not differ among the three groups. (*B*) Mean wall thickness was increased in CLE compared with control subjects and PLE. (*C*) Wall volume and total airway volume were reduced in CLE and PLE compared with control subjects. (*D* and *E*) Coefficients of variation (CV%) of luminal area and wall thickness within and between bronchioles in which greater variation was found in CLE than control subjects and PLE. *Boxplots* indicate the median value (*horizontal line*) and the interquartile range (*box*). *Adjusted P value < 0.05.

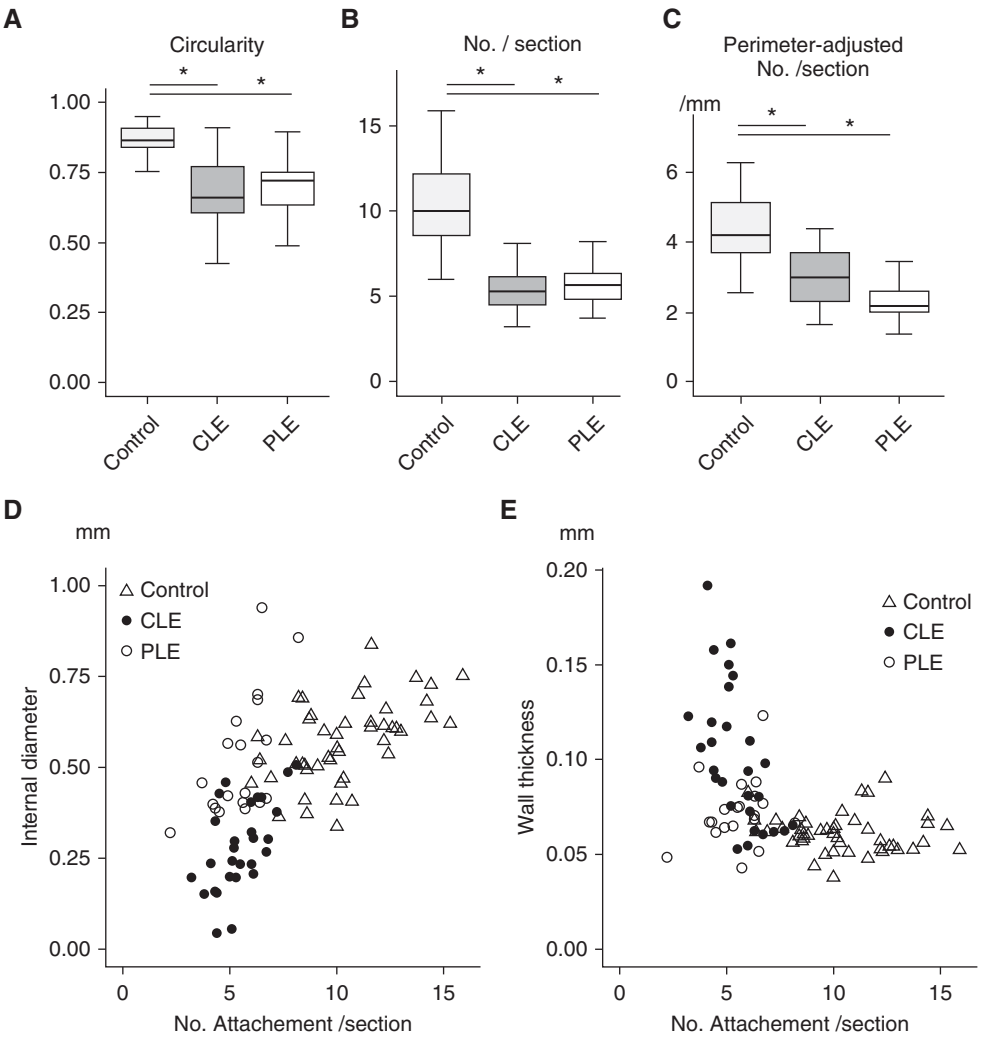

Figure 4. Compares preterminal bronchiolar lumen shape and numbers of alveolar attachments to the outer walls of the airways. (*A*) Circularity of the lumen, (*B*) numbers of alveolar attachments, and (*C*) reduction in the numbers of attachments per length of outer airway wall circumference in centrilobular (CLE) and panlobular (PLE) emphysema compared with control subjects. (*D*) Reduction in number of attachments is associated with reduced internal diameter in CLE (*solid circles*, standardized beta [β^*] = 0.59, $P = 0.0006$), PLE (*open circles*, $\beta^* = 0.62$, $P = 0.002$) and control subjects (*open triangles*, $\beta^* = 0.72$, $P = 0.000004$). (*E*) Reduction in numbers of attachments is associated with the greater wall thickness only in CLE ($\beta^* = -0.60$; $P = 0.0008$). *Boxplots* indicate the median value (*horizontal line*) and the interquartile range (*box*). *Adjusted *P* value < 0.05.

infiltration or the formation of tertiary lymphoid organs in explanted lungs removed from patients treated by lung transplantation. It remains to be investigated how the inflammatory response drives similar and different structural consequences between the phenotypes.

The analysis of the preterminal bronchioles reported here represents a first step toward the ultimate goal of understanding the nature of small airway disease from the approximately 2 mm in diameter airways visible on MDCT to the terminal and respiratory bronchioles only visible on microCT and histology. The size of tissue samples used in this study was not large enough to analyze airways more proximal to preterminal bronchioles. To identify these airways, tissue samples should include not only the target airways but also the terminal bronchiole subtended by those airways because this is the last conducting airway and allows airway generation to be attributed to all proximal airways. A method of scanning larger tissue samples needs to be established to conduct such studies.

The current study used a subset of samples that included at least one whole preterminal bronchiole. Such a subsampling could generate a regional bias between the groups. Figure E4A demonstrates that samples with preterminal bronchioles were evenly distributed from the apex to base in the lungs of control subjects and patients with CLE, whereas samples with preterminal bronchioles from patients with PLE were predominantly located in the upper regions of the lung. Because lower regions of lung with PLE were so severely destroyed, the chance to find complete preterminal bronchiole was reduced. To test for regional bias we performed a subanalysis of upper and lower regions of the lungs separately. Although the number of samples with PLE in the lower regions was too small (n = 3) to perform statistical

Table 3. Associations between Small Airway Disease Parameters and Measures of Emphysema and Alveolar Attachments

	Control Subjects (*n* = 47)	Centrilobular Emphysema (*n* = 28)	Panlobular Emphysema (*n* = 20)
Alveolar attachment vs. internal diameter	0.72*	0.59*	0.62*
Alveolar attachment vs. circularity	0.58	0.68*	0.50†
Alveolar attachment vs. wall thickness	0.17	−0.60*	−0.16
Adjusted attachment vs. wall thickness	−0.25	−0.62*	−0.08
Lm vs. wall thickness	0.04	0.11	0.12

Definition of abbreviations: adjusted attachment = mean number of alveolar attachment per cross-section adjusted by outer perimeter of the bronchiole; alveolar attachment = mean number of alveolar attachment per cross-section; circularity = circularity of lumen of preterminal bronchiole; Lm = mean of interalveolar wall distances.
"X versus Y" indicates that X and Y are independent and dependent variables, respectively, in a linear mixed-effects model that includes cases as a random effect. Each value represents standardized beta coefficient (β*) in the model.
*$P < 0.01$.
†$P < 0.05$.

comparisons, similar reductions of bronchiolar length and wall volume were found in PLE in the upper and lower regions (*see* Figure E4B). These data suggest that the different distributions of cores with PLE have little impact on the current findings.

The subjects' demographic data (Table 1) show that all patients with PLE associated with alpha-1 antitrypsin deficiency were former smokers, although their pack-years of cigarette smoking were less than patients with CLE (*see* Section E2–2).

The inner and outer borders of the preterminal bronchioles were measured using the full width at half-maximum principle, which has been validated by histology in studies where airways approximately 2 mm in diameter and larger were examined (12, 37). To compare airway WT measured by microCT with that measured by histology, we used the record of airway WT previously measured by histology in samples adjacent to those scanned with microCT (17). These data show that in 19 pairs of samples, the WT measured by histology is comparable with the thickness measured by microCT (*see* Figure E5). In addition, the present results are consistent with several previous histologic analyses of small airways (2, 4, 34, 38) that showed greater WT in CLE than in control subjects and PLE. This concordance of results strongly supports the validity of the methodology.

The major advantage of X-ray over light microscopy is that X-ray-based CT (i.e., microCT) provides three-dimensional information about tissue structure that is difficult to obtain with light microscopy. However, this comes with the disadvantage that microCT produces less contrast than light microscopic histology at similar magnifications (26). Although this introduces a potential source of error that could affect measurements lumen area and WT, these errors are probably small. MicroCT provides much greater accuracy in measuring a preterminal bronchiole than MDCT in measuring a 2 mm in diameter airway. The ratio of the 10- to 16-μm in-plane spatial resolution of the microCT used in this study to the 500-μm lumen diameter of the target preterminal bronchiole is 0.02–0.03, whereas the ratio of the in-plane 600- to 800-μm spatial resolution of MDCT scan to the 2-mm airway (2,000 μm) target airway ranges from 0.3 to 0.4. This means that microCT provides an approximate 100-fold increase in accuracy over MDCT. That is reflected in the comparison between microCT and histology (*see* Figure E5), where the WT measured by microCT (89.5 ± 29.7 μm) was not different from WT measured by histology (90.2 ± 38.8 μm). Another potential source of error is that samples were imaged at different resolutions (10, 11, and 16 μm per voxel) with different microCT scanners (*see* Section E2–3).

Although the number of cases examined in the present study was small and the pathology of COPD is heterogeneous (17, 39), sampling several cores from different regions of each lung allowed us to evaluate the microstructure of regions at different levels of tissue destruction. Multiple sampling from each individual and the use of mixed-effects models that allowed the lungs to be included as a random effect enhanced the validity of the present results.

Based on these new data, we conclude that the preterminal bronchioles are extensively damaged in both centrilobular and panlobular phenotypes of emphysematous destruction and that the nature of these abnormalities is different in these two conditions. In future studies, we plan to extend this methodology to all of the lobular airways and begin to link them to molecular determinants associated with different pathologic phenotypes of COPD. ■

Author disclosures are available with the text of this article at www.atsjournals.org.

References

1. Hogg JC. Pathophysiology of airflow limitation in chronic obstructive pulmonary disease. *Lancet* 2004;364:709–721.
2. Hogg JC, Chu F, Utokaparch S, Woods R, Elliott WM, Buzatu L, Cherniack RM, Rogers RM, Sciurba FC, Coxson HO, *et al*. The nature of small-airway obstruction in chronic obstructive pulmonary disease. *N Engl J Med* 2004;350:2645–2653.
3. Lynch DA, Austin JH, Hogg JC, Grenier PA, Kauczor HU, Bankier AA, Barr RG, Colby TV, Galvin JR, Gevenois PA, *et al*. CT-definable subtypes of chronic obstructive pulmonary disease: a statement of the Fleischner Society. *Radiology* 2015;277:192–205.
4. Kim WD, Eidelman DH, Izquierdo JL, Ghezzo H, Saetta MP, Cosio MG. Centrilobular and panlobular emphysema in smokers. Two distinct morphologic and functional entities. *Am Rev Respir Dis* 1991;144: 1385–1390.
5. Saetta M, Kim WD, Izquierdo JL, Ghezzo H, Cosio MG. Extent of centrilobular and panacinar emphysema in smokers' lungs: pathological and mechanical implications. *Eur Respir J* 1994;7: 664–671.
6. Smith BM, Austin JH, Newell JD, Jr., D'Souza BM, Rozenshtein A, Hoffman EA, Ahmed F, Barr RG. Pulmonary emphysema subtypes on computed tomography: the MESA COPD study. *Am J Med* 2014;127:94.

7. Kim WD, Ling SH, Coxson HO, English JC, Yee J, Levy RD, Paré PD, Hogg JC. The association between small airway obstruction and emphysema phenotypes in COPD. *Chest* 2007;131:1372–1378.
8. Coxson HO. Quantitative chest tomography in COPD research: chairman's summary. *Proc Am Thorac Soc* 2008;5:874–877.
9. Castaldi PJ, San José Estépar R, Mendoza CS, Hersh CP, Laird N, Crapo JD, Lynch DA, Silverman EK, Washko GR. Distinct quantitative computed tomography emphysema patterns are associated with physiology and function in smokers. *Am J Respir Crit Care Med* 2013; 188:1083–1090.
10. Hasegawa M, Nasuhara Y, Onodera Y, Makita H, Nagai K, Fuke S, Ito Y, Betsuyaku T, Nishimura M. Airflow limitation and airway dimensions in chronic obstructive pulmonary disease. *Am J Respir Crit Care Med* 2006;173:1309–1315.
11. Nakano Y, Muro S, Sakai H, Hirai T, Chin K, Tsukino M, Nishimura K, Itoh H, Paré PD, Hogg JC, *et al*. Computed tomographic measurements of airway dimensions and emphysema in smokers. Correlation with lung function. *Am J Respir Crit Care Med* 2000;162: 1102–1108.
12. Nakano Y, Wong JC, de Jong PA, Buzatu L, Nagao T, Coxson HO, Elliott WM, Hogg JC, Paré PD. The prediction of small airway dimensions using computed tomography. *Am J Respir Crit Care Med* 2005;171:142–146.
13. Solomon J, Wilson J, Samei E. Characteristic image quality of a third generation dual-source MDCT scanner: noise, resolution, and detectability. *Med Phys* 2015;42:4941–4953.
14. Newell JD Jr, Fuld MK, Allmendinger T, Sieren JP, Chan KS, Guo J, Hoffman EA. Very low-dose (0.15 mGy) chest CT protocols using the COPDGene 2 test object and a third-generation dual-source CT scanner with corresponding third-generation iterative reconstruction software. *Invest Radiol* 2015;50:40–45.
15. Galbán CJ, Han MK, Boes JL, Chughtai KA, Meyer CR, Johnson TD, Galbán S, Rehemtulla A, Kazerooni EA, Martinez FJ, *et al*. Computed tomography-based biomarker provides unique signature for diagnosis of COPD phenotypes and disease progression. *Nat Med* 2012;18:1711–1715.
16. Boes JL, Hoff BA, Bule M, Johnson TD, Rehemtulla A, Chamberlain R, Hoffman EA, Kazerooni EA, Martinez FJ, Han MK, *et al*. Parametric response mapping monitors temporal changes on lung CT scans in the Subpopulations and Intermediate Outcome Measures in COPD Study (SPIROMICS). *Acad Radiol* 2015;22:186–194.
17. McDonough JE, Yuan R, Suzuki M, Seyednejad N, Elliott WM, Sanchez PG, Wright AC, Gefter WB, Litzky L, Coxson HO, *et al*. Small-airway obstruction and emphysema in chronic obstructive pulmonary disease. *N Engl J Med* 2011;365:1567–1575.
18. Yushkevich PA, Piven J, Hazlett HC, Smith RG, Ho S, Gee JC, Gerig G. User-guided 3D active contour segmentation of anatomical structures: significantly improved efficiency and reliability. *Neuroimage* 2006;31:1116–1128.
19. Schneider CA, Rasband WS, Eliceiri KW. NIH Image to ImageJ: 25 years of image analysis. *Nat Methods* 2012;9:671–675.
20. Lee TC, Kashyap RL, Chu CN. Building skeleton models via 3-D medial surface axis thinning algorithms. *Computer Vision, Graphics, and Image Processing* 1994;56:462–478.
21. Hsia CC, Hyde DM, Ochs M, Weibel ER; ATS/ERS Joint Task Force on Quantitative Assessment of Lung Structure. An official research policy statement of the American Thoracic Society/European Respiratory Society: standards for quantitative assessment of lung structure. *Am J Respir Crit Care Med* 2010;181:394–418.
22. Washko GR, Dransfield MT, Estépar RS, Diaz A, Matsuoka S, Yamashiro T, Hatabu H, Silverman EK, Bailey WC, Reilly JJ. Airway wall attenuation: a biomarker of airway disease in subjects with COPD. *J Appl Physiol (1985)* 2009;107:185–191.
23. Nagai A, Yamawaki I, Takizawa T, Thurlbeck WM. Alveolar attachments in emphysema of human lungs. *Am Rev Respir Dis* 1991;144: 888–891.
24. Saetta M, Ghezzo H, Kim WD, King M, Angus GE, Wang NS, Cosio MG. Loss of alveolar attachments in smokers. A morphometric correlate of lung function impairment. *Am Rev Respir Dis* 1985;132:894–900.
25. Petty TL, Silvers GW, Stanford RE. Radial traction and small airways disease in excised human lungs. *Am Rev Respir Dis* 1986;133: 132–135.
26. Vasilescu DM, Klinge C, Knudsen L, Yin L, Wang G, Weibel ER, Ochs M, Hoffman EA. Stereological assessment of mouse lung parenchyma via nondestructive, multiscale micro-CT imaging validated by light microscopic histology. *J Appl Physiol (1985)* 2013; 114:716–724.
27. R Core Team. R: a language and environment for statistical computing. 2015 [accessed 2015 Dec 15]. Available from: http://www.R-project.org/
28. Bates D, Mächler M, Bolker MB, Walker SC. Fitting linear mixed-effects models using lme4. *J Stat Softw* 2015;67:1–48.
29. Hothorn T, Bretz F, Westfall P. Simultaneous inference in general parametric models. *Biom J* 2008;50:346–363.
30. Mitzner W. Emphysema: a disease of small airways or lung parenchyma? *N Engl J Med* 2011;365:1637–1639.
31. Macklin CC. A note on the elastic membrane of the bronchial tree of mammals, with an interpretation of its functional significance. *Anat Rec* 1922;24:119.
32. Anderson AE Jr, Hernandez JA, Eckert P, Foraker AG. Emphysema in lung macrosections correlated with smoking habits. *Science* 1964; 144:1025–1026.
33. Hogg JC, McDonough JE, Suzuki M. Small airway obstruction in COPD: new insights based on micro-CT imaging and MRI imaging. *Chest* 2013;143:1436–1443.
34. Willems LN, Kramps JA, Stijnen T, Sterk PJ, Weening JJ, Dijkman JH. Relation between small airways disease and parenchymal destruction in surgical lung specimens. *Thorax* 1990;45:89–94.
35. Ballarin A, Bazzan E, Zenteno RH, Turato G, Baraldo S, Zanovello D, Mutti E, Hogg JC, Saetta M, Cosio MG. Mast cell infiltration discriminates between histopathological phenotypes of chronic obstructive pulmonary disease. *Am J Respir Crit Care Med* 2012; 186:233–239.
36. Baraldo S, Turato G, Lunardi F, Bazzan E, Schiavon M, Ferrarotti I, Molena B, Cazzuffi R, Damin M, Balestro E, *et al*. Immune activation in α1-antitrypsin-deficiency emphysema. Beyond the protease-antiprotease paradigm. *Am J Respir Crit Care Med* 2015;191: 402–409.
37. Paré PD, Nagano T, Coxson HO. Airway imaging in disease: gimmick or useful tool? *J Appl Physiol (1985)* 2012;113:636–646.
38. Leopold JG, Gough J. The centrilobular form of hypertrophic emphysema and its relation to chronic bronchitis. *Thorax* 1957;12: 219–235.
39. Campbell JD, McDonough JE, Zeskind JE, Hackett TL, Pechkovsky DV, Brandsma CA, Suzuki M, Gosselink JV, Liu G, Alekseyev YO, *et al*. A gene expression signature of emphysema-related lung destruction and its reversal by the tripeptide GHK. *Genome Med* 2012;4:67.